[Mansoura Engineering Journal](https://mej.researchcommons.org/home)

Volume 49 | Issue 3 Article 11

2024

Effect of the Shape and Volume of Capsulated Phase Change Materialon the Melting Process and Exergy Efficiency

Ahmed Saad Soliman
Mechanical Power Engineering Department, Mansoura University, El-Mansoura, 35516, Egypt

Ahmed A. Sultan
Mechanical Power Engineering Department, Mansoura University, El-Mansoura, 35516, Egypt, aasultan@mans.edu.eg

Mohamed A. Sultan
Mechanical Engineering Department, Higher Future Institute of Engineering and Technology, El-Mansoura 35516, Egypt

ORIGINAL STUDY

Effect of the Shape and Volume of Capsulated Phase Change Material on the Melting Process

Ahmed S. Soliman [a], Ahmed A. Sultan [a,*], Mohamed A. Sultan [b]

[a] Department of Mechanical Power Engineering, Mansoura University, Egypt
[b] Department of Mechanical Engineering, Higher Future Institute of Engineering and Technology, El-Mansoura, Egypt

Abstract

Due to the lack of continuity in solar energy throughout the day, researchers tend to store this energy in phase change materials (PCM). The goal is to store a big amount of energy in a small PCM mass. In this study, the effect of the capsule shape (circular and elliptical cross-section), number of capsules with the same volume (1, 2, 3, 4, and 5 capsules), and one capsule with increasing its initial volume (multiplying of volume ratio 1 ($V_r = 2, 3, 4$, and 5)) on the PCM melting process was studied. The results of the numerical model for both circular and elliptical cross-section capsules are validated with the experimental results in the literature and have a good agreement. The results concluded that the performance of the elliptical cross-section capsule is higher than that of the circular cross-section at the same area, which leads to a decrease in the melting time by up to 50 % for the same amount of heat stored in the capsule. The V_r value has a great impact on the numerical results of the PCM melting process. The capsule melting time and its total energy stored increased as the value of V_r raises. The exergy difference between the two configurations increases with the increase of the volume ratio and number of capsules. The exergy efficiency of the capsule with a volume ratio equal to 5 is the highest value among all the discussed capsules (18.5 %).

Keywords: Energy storage, Horizontal elliptical capsules, Heat transfer fluid, Volume ratio

1. Introduction

Nowadays, researchers are interested in solving the problem of the depletion of traditional energy sources such as coal and petroleum. Thus, they turned to the use of new and renewable energy represented in wind energy, wave energy, and solar energy, all of which are not available at all times. Therefore, researchers tend to store this energy when it is available to use it when it is not. This energy can be stored in various forms, such as mechanical energy, electrical energy, and thermal energy. Both mechanical and electrical energy need a process of converting the energy available to it using specific devices that occupy a large space and have a high cost to store weak levels of energy. Solar energy is a clean and renewable source of energy that has the potential to meet most of our future energy needs with minimal environmental impact (Goswami, 2022). Thermal energy storage devices are essential for reducing our reliance on fossil fuels and making solar energy more accessible and reliable (Dinçer and Rosen, 2010). Considering that solar energy is one of the most important energies available all over the world throughout the year and in large quantities, researchers have been interested in ways to store solar energy when it is available and use it when it is not. One of the common ways to store solar energy is to store it in the form of thermal energy when it is available in phase change materials (PCMs) by adding the latent heat of its fusion and converting it from the solid form to the liquid form and then reusing it when it is not available by expelling the latent heat by converting it from the liquid form to the solid form again.

The main challenge is how to quickly and efficiently store enormous amounts of energy in a small mass of PCM as well. For this purpose, containers

Received 1 November 2023; revised 3 January 2024; accepted 5 January 2024.
Available online 1 March 2024

* Corresponding author at: Mechanical Power Engineering Department, Mansoura University, El-Mansoura, 35516, Egypt.
E-mail address: aasultan@mans.edu.eg (A.A. Sultan).

https://doi.org/10.58491/2735-4202.3182

for charging the PCMs were used in different shapes and sizes to reach the minimum storage time and the least amount of the phase-change material to store a certain amount of thermal energy.

Several capsule shapes such as spherical capsules (Dzikevics et al., 2016), cylindrical capsules with a circular section (Dhaidan et al., 2013), and another cross-section area (Soliman et al., 2022a) were used. Some investigations used capsules of small size to enhance the process of melting and solidification such as microcapsules (Jamekhorshid et al., 2014), and nano-capsules (Sabbaghi and Mehravar, 2015). The researchers used heat exchangers of different types, for example, a tube-in-tube type where the phase change material was charged inside the inner tube and the heat transfer fluid was flowing through the space between the inner and outer tubes (Kapilow et al., 2018; Pirasaci et al., 2017). Some researchers investigated the melting of PCM inside an annular-shaped heat exchanger where the inside tube was charged with PCM while the heat transfer fluid (HTF) was flowing through the annular passage between the two tubes (Kothari et al., 2019; Li et al., 2017). Also, shell-and-tube heat exchangers have been used so that the PCM was charged inside the tubes and the heat-transfer material was flowing in the space between the tubes (Li et al., 2021). Investigations included a heat exchanger in the form of a shell and a spiral tube so that the HTF was flowing inside the spiral tube and the PCM was charged in the space between the spiral tube and the shell (Mahdi et al., 2019). The melting process of the paraffin wax in a multi-tube energy storage system was studied at different configurations of the heat transfer fluid tubes with radial eccentricity. The melting process was greatly changed by the HTF tube arrangement. To prevent thermal stratification, the tubes in the top half of the shell should be placed closer to the center, while the tubes in the bottom half of the shell should be positioned further into the poor melting zone (Vikas et al., 2022). The melting and solidification process of PCM (paraffin wax) was investigated numerically, and the results were compared with the experimental results. The heat exchanger unit storage consisted of an epoxy resin loaded with metal hollow tubes filled with paraffin wax. The graphite and metal tubes were used to improve the heat transfer rate and played an effective role. The Paraffin wax can be used to enhance comfort, and save energy in buildings (Aadmi et al., 2015; Soliman et al., 2023). A triplex tube was used as an energy storage system where the PCM was charged inside the middle annulus while the HTF was flowing through the inner tube and/or the outer annulus (Ali et al., 2022).

Nomenclature

A_{mush}	mushy zone constant (kg/m^3.s)
C_p	specific heat capacity (J/kg. K)
D	capsule diameter (m)
g	gravitational acceleration (m/s^2)
H	specific enthalpy (J/kg)
λ	liquid fraction (%)
μ	dynamic viscosity (Pa. s)
α	thermal diffusivity (m^2/s)
ρ_l	liquid density (kg/m^3)
ρ_s	solid density (kg/m^3)
h	specific sensible enthalpy (J/kg)
h_{ref}	reference-specific enthalpy (J/kg)
k	thermal conductivity (W/m.K)
L	latent heat of melting (J/kg)
S	momentum source term (pa/m)
T	temperature (K)
t	time (s)
T_s	solidus temperature (K)
T_l	liquidus temperature (K)

Greek symbols

β	thermal expansion coefficient (1/K)

Abbreviations

CFD	computational fluid dynamics
CPVC	chlorinated polyvinyl chloride
EPCM	encapsulated PCM
HTF	heat transfer fluid
LHTES	latent heat thermal energy storage
PCM	phase change material
V_r	volume ratio

To reduce the time required to store energy by improving the charging process of the PCM, researchers used various methods, including the use of fins inside the PCM (Pássaro et al., 2022), or the use of nanoparticles added to the PCM to advance the heat transfer process (Soliman et al., 2021a, 2021b). To adjust the HTF temperature under a certain level of stored energy, some researchers investigated the use of capsules of multi-layer PCM of different types (Soliman et al., 2022b). A theoretical investigation has been carried out to investigate the heat exchanger thermal performance containing several oval tubes and a cylindrical shell of a heat exchanger filled with the PCM. Four and two fins are added to the perimeter of the elliptical tubes to improve heat transfer from them to the PCM (Rana et al., 2022).

A computational investigation was made on the constrained paraffin wax as PCM inside an elliptical cross-section cell under the effect of variable wall heat fluxes is presented. The effect of prolate and oblate capsules on the melting front transient movement and the liquid fraction is discussed (Dhaidan, 2021).

Two theoretical studies have been carried out to study the paraffin wax melting process charged in a capsule with a horizontal axis and its section in the form of an ellipse (Sultan et al., 2021). The capsule was placed with the larger axis of the ellipse in a direction perpendicular to the gravitational acceleration (horizontal) and the smaller axis in the direction of it (vertical). The effect of changing the inlet temperature of the heat transfer fluid from 334 K to 343 K and its velocity from 0.003 m/s to 0.012 m/s was studied, while the ratio of the two axes was changed from 0.2 to 6.25. The effect of the inlet velocity of the heat transfer fluid on the melting process is very weak, while the effect of the temperature of the heat transfer fluid is significant, followed by the effect of the axe's ratio. By comparing the results of the two studies, it was found that the melting time of the capsule whose largest cross-section axis is horizontal is less than that whose largest cross-section axis is vertical.

Melting of a nano-enhanced phase change material (NEPCM) dispersed with Cu nanoparticles in partially filled horizontal elliptical capsules is investigated numerically (Hajighafoori Boukani et al., 2018). The geometry of the physical model is a horizontal elliptical capsule having constant heat flux on the surface and partially filled with PCM. Three different aspect ratios are examined. Three volumetric concentrations (0, 1, and 3 vol%) of nanoparticles were used.

From the published research available to current researchers, the following observations can be reached:

First, several investigations used spherical capsules single or within packed-bed type heat exchangers with different diameters and charged with different PCMs. Second, in the research that dealt with cylindrical capsules, most of them had a circular section, and a small group of them focused on changing the shape of the cylinder cross-section to improve the heat transfer coefficient and thus reach a melting time as little as possible with the amount of heat stored as much as possible.

Third, the number of investigations that dealt with capsules with elliptical cross sections is small. Fourth, the available research that used horizontal cylinders whose section was in the form of an ellipse, assumed the surface of the capsule was exposed to a constant heat flux or a constant temperature with no moving fluid around it. Also, they used a tube in the form of an ellipse through which the HTF flows, while the PCM was found in the annular space.

In the available literature, there was no study dealing with the effect of changing the dimensions of the capsules on the rate of energy stored or released and the efficiency of the system. Accordingly, the novelty of the present research is the use of capsules in the form of a horizontal cylinder whose section is in the form of an ellipse subjected to a cross-flow of the HTF (water). Also, the study explores the effect of capsules' cross-sectional area and the volume ratio of the PCM (paraffin wax) that was charged inside it on the melting process. In addition, the exergy efficiency is calculated to get the highest thermal performance between the studied cases of the energy storage system.

The optimum design from the present work would help the researchers store a large amount of energy in a small PCM mass with high energy and exergy efficiency.

2. Physical model

The computational domain of the present work is shown in Table 1. In the current study, the capsule is filled with a PCM (paraffin wax) in the solid phase. Hence, the volume should increase during the melting process. The capsules are surrounded by water, which can provide heat to the capsules. The studied cases are divided into four parts: circular capsule, oval horizontal capsule, different numbers of oval capsule, and different volume ratios (V_r) of a single oval capsule.

The melting of paraffin wax in capsules is a complex process that is affected by several factors, including the capsule shape, capsule material, PCM material, melting conditions, and boundary conditions. By studying the melting of paraffin wax in capsules under different conditions, we can gain a better understanding of the underlying physics of the process and develop more accurate and predictive models, furthermore, developing better designs for PCM-based thermal energy storage devices. For the circular capsule, this case is the simplest, and it allows for the study of the fundamental physics of the melting process. For the oval horizontal capsule, this case allows for the study of the effect of capsule shape on the melting process. For the different capsule numbers, this case allows for the study of the interaction between neighboring capsules during the melting process. For the different V_r, this case allows for the study of the effect of the volume ratio of one capsule on the melting process, compared with the same volume but when using several numbers of capsules.

The PCM capsules lay with their centerline horizontal and had elliptical cross sections of two axes a and b, an insulated duct of height and width depending on the smallest and largest axes (a and b) as shown in Table 2, with a length of 1 m is used.

Table 1. Studied cases of capsules in the present work.

Circular capsule	Oval capsule	Different volume ratio	Different capsule numbers
		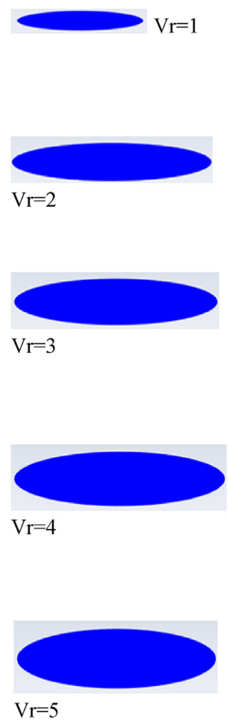	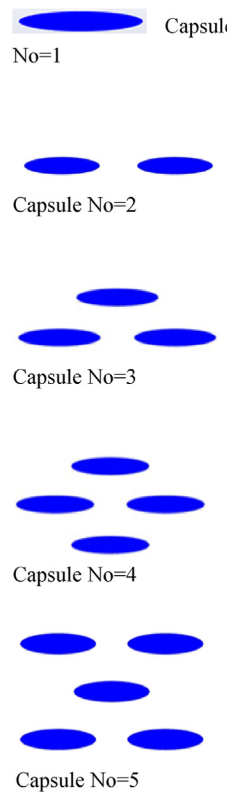

The elliptical cross-sectional capsule is surrounded by the HTF that interacts with the tank top component in the antigravity direction. The HTF is water, while the PCM is paraffin wax and Table 3 lists the PCM's (paraffin wax) thermal properties. The inlet HTF temperature is kept constant above the PCM melting temperature throughout the PCM charging (melting) process.

3. Numerical model

The objective of the numerical model used in this study is to examine the numerous variables that influence how PCMs inside capsules placed horizontally through the flow route melt. Using the ANSYS Fluent 2019 R2, the numerical simulation of a two-dimensional mathematical transient melting model for PCM is performed. The upcoming work makes the following presumptions.

(1) It is considered that heat transfer occurs in two dimensions.

Table 2. Dimensions of heat transfer duct at different capsule numbers.

Capsule number	1	2	3	4	5
Height, cm	15	15	15	15	15
Width, cm	15	20	20	30	30

Table 3. Phase change material's thermophysical properties (Soliman et al., 2021c).

Thermophysical properties	Paraffin wax
K_s (W/m.K)	0.15
K_l (W/m.K)	0.15
ρ_s (kg/m^3)	890
ρ_l (kg/m^3)	712
$C_{P\,s}$ (kJ/kg. K)	2.384
$C_{P\,l}$ (kJ/kg. K)	2.44
Kinematic viscosity (m^2/s)	8.31×10^{-5}
Melting temperature (°C)	54.22/56.22
Latent heat (kJ/kg)	278.8
Thermal exp. coeff (l/k)	0.000714

(2) PCM is a pure compound, and the capsules' solid walls are isotropic.
(3) The heat transfer fluid and the capsuled PCM are placed in a cross-flow.
(4) The 2-D sides' heat transfer was disregarded.
(5) Under conditions of laminar flow, molten PCM and the heat transfer fluid cannot undergo compressible movement.

To model the combined heat transfer and phase change, the enthalpy porosity method was used. In this method, the solid–liquid interface is not tracked explicitly. Instead, the mushy zone (the region where both solid and liquid phases are present) is treated as a porous medium. Momentum sink terms are applied to the momentum equations in the mushy zone to account for the pressure drop caused by the presence of solid material (Soliman et al., 2021d). The difference in density of the PCM in the buoyancy term is modeled using the Boussinesq approximation, which accounts for thermal buoyancy. The buoyancy-driven conventional governing equations contained in the 2-D transient model are as follows:

The continuity equation

$$\frac{\partial \rho}{\partial t}+\frac{1}{r}\frac{\partial (r\rho V_r)}{\partial r}+\frac{1}{r}\frac{\partial (\rho V_\theta)}{\partial \theta}=0 \tag{1}$$

The momentum equations:

Momentum r:

$$\begin{aligned}\rho\left(\frac{\partial (V_r)}{\partial t}+V_r\frac{\partial (V_r)}{\partial r}+\frac{V_\theta}{r}\frac{\partial (V_r)}{\partial \theta}-\frac{V_\theta^2}{r}\right)&=-\frac{\partial P}{\partial r}\\ &+\mu\left[\frac{1}{r}\frac{\partial}{\partial r}\left(r\frac{\partial (V_r)}{\partial r}\right)-\frac{V_r}{r^2}+\frac{1}{r^2}\frac{\partial^2 (V_r)}{\partial \theta^2}-\frac{2}{r^2}\frac{\partial (V_\theta)}{\partial \theta}\right]\\ &+\rho g\beta(\mathrm{T}-\mathrm{T_m})+S\end{aligned} \tag{2}$$

Momentum θ:

$$\rho\left(\frac{\partial (V_\theta)}{\partial t}+V_r\frac{\partial (V_\theta)}{\partial r}+\frac{V_\theta}{r}\frac{\partial (V_\theta)}{\partial \theta}+\frac{V_rV_\theta}{r}\right)=-\frac{1}{r}\frac{\partial P}{\partial \theta}+\mu\left[\frac{1}{r}\frac{\partial}{\partial r}\left(r\frac{\partial (V_\theta)}{\partial r}\right)-\frac{V_\theta}{r^2}+\frac{1}{r^2}\frac{\partial^2 (V_\theta)}{\partial \theta^2}-\frac{2}{r^2}\frac{\partial (V_r)}{\partial \theta}\right]+S \tag{3}$$

The parameter S is Darcy's law damping term that was added to the momentum equation due to the impact of the convective phase change. This term depends on both the mushy zone constant A_{mush} and the liquid fraction (λ), which can be expressed as follows:

$$\vec{S}=\frac{(1-\lambda)^2}{(\lambda^3+\gamma)}A_{\mathrm{mush.}}\vec{V}$$

where γ is a small number usually about 10^{-3} applied to prevent division by zero in the damping term of Darcy's law. The mushy zone constant A_{mush} value is high and can be nominated between 10^4 and 10^8. In the present study, A_{mush} is defined to be 10^6. Different investigations recommended considering the A_{mush} value equal to 106, which gives the best match between the experimental and numerical outcomes (Soliman, 2023).

The energy equation

$$\frac{\partial h}{\partial t}+\frac{\partial H}{\partial t}+\nabla\cdot\left(\vec{V}h\right)=\nabla\cdot\left(\frac{k}{\rho c_p}\nabla h\right) \tag{4}$$

The H factor defines the PCM enthalpy and the h1 parameter is the value of the sensible enthalpy, and the latent heat is expressed by ΔH (Soliman et al., 2022c):

$$H=h_1+\Delta H \tag{5}$$

$$h_1=h_{ref}+\int_{T_{ref}}^{T} Cp\,dT \tag{6}$$

where h_{ref} is the reference enthalpy at the reference temperature of T_{ref} and the term of latent heat can be stated as a function of the total PCMs latent heat (L) as follows:

$$\Delta H=\lambda L \tag{7}$$

where ΔH varies from L (liquid) to zero (solid). So, the liquid fraction λ can be expressed by the following equation (Abo-Elnour et al., 2023):

$$\lambda = \begin{cases} \frac{\Delta H}{L} = 0 \; T < T_m \\ \frac{\Delta H}{L} = \frac{T - T_{solidus}}{T_{liqudus} - T_{solidus}} T_m < T < T_m + \Delta T_m \\ \frac{\Delta H}{L} = 1 \; T > T_m + \Delta T_m \end{cases} \quad (8)$$

The ΔT_m parameter can be expressed as the change between the temperature values of the PCM liquid and solid phases:

$$\Delta T_m = T_{liquidus} - T_{solidus} \quad (9)$$

The PCM density and thermal conductivity are expressed by the following equations:

$$\rho_{pcm} = \begin{cases} \rho_s \; T < T_m \\ \frac{\rho_s + \rho_l}{2} T_m < T < T_m + \Delta T_m \\ \rho_l \; T > T_m + \Delta T_m \end{cases} \quad (10)$$

$$k_{pcm} = \begin{cases} k_s \; T < T_m \\ \frac{k_s + k_l}{2} T_m < T < T_m + \Delta T_m \\ k_l \; T > T_m + \Delta T_m \end{cases} \quad (11)$$

The exergy balance for a typical LHTS system during the charging process is illustrated in Fig. 1.

The related expressions for the charging process suggested as mentioned in Ref (Jegadheeswaran et al., 2010) are as follows:

Exergy input:

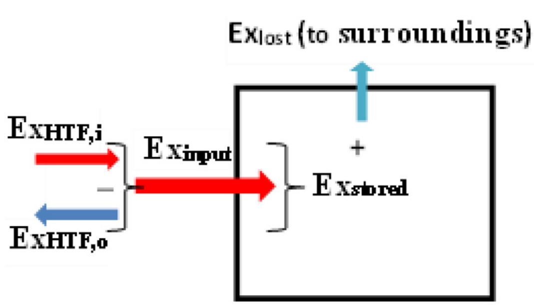

Fig. 1. Exergy balance for a typical LHTS System during the charging process.

$$\dot{Ex}_{in\,put} = \dot{m}_{HTF} c_{HTF} \left[(T_{HTF,in} - T_{HTF,out}) - T_0 \ln \left(\frac{T_{HTF,in}}{T_{HTF,out}} \right) \right] \quad (12)$$

Exergy stored:

$$\dot{Ex}_{stord} = ML \left[1 - \left(\frac{T_0}{T_m} \right) \right] + Mc_{PCM,S} \left[(T_{PCM,init} - T_m) - T_0 \ln \left(\frac{T_{PCM,init}}{T_m} \right) \right] + Mc_{PCM,l} \left[(T_m - T_{PCM,final}) - T_0 \ln \left(\frac{T_m}{T_{PCM,final}} \right) \right] \quad (13)$$

Exergy input:

$$\dot{Ex}_{output} = \dot{m}_{HTF} c_{HIF} \left[(T_{HTF,out} - T_{HTF,in}) - T_o \ln \left(\frac{T_{HTF,out}}{T_{HTF,in}} \right) \right] \quad (14)$$

Watanabe and Kanzawa (1995) expressed the exergy efficiency as follows:

$$\Psi \text{ch} = \frac{\text{PCM stored Exergy}}{\text{HTF supplied Exergy}} \quad (15)$$

Since the heat transfer in LHTS systems is time dependent, the evaluation of the exergy efficiency during melting at any time is also important. This motivates us to determine the exergy efficiency in the shape of the exergy rate.

$$\Psi \text{ch} = \frac{\text{The PCM exergy stored rate}}{\text{HTF supplied Exergy}} \quad (16)$$

Thus, Rosen and Dincer (2003) had informed that the pumping power to handle the HTF must be taken into account in the evaluation of exergy efficiency. They proved that the difference between the exergy efficiency that considers the pumping power and that neglects it is considerable. Moreover, this variance is more studied in the case of exergy efficiency than in the case of energy efficiency.

Ozturk (Öztürk, 2005) gave an exergy efficiency expression that considers the pumping power which is given below:

$$\Psi\text{char} = \frac{\text{The PCM exergy stored rate}}{\text{The HTF supplied exergy rate} + \text{Mechanical power input to HTF}} \tag{17}$$

3.1. Boundary and initial conditions

At the start, the capsule wall as well as the solid PCM temperature is 302 K. Also, at the solid–liquid interface no-slip boundary conditions are considered. The flow regime is considered laminar for both water and PCM, as well as an adiabatic boundary condition is assumed for the two side walls of the test section. But, at the inlet section, the inlet velocity boundary condition is applied under a specific inlet temperature. Finally, at the outlet section pressure boundary conditions are applied and at the interfaces, thermally coupled boundary conditions are assumed as shown in Fig. 2. Model validation with experimental data and the Mesh independence test of this study are presented in the supplementary data.

3.2. Numerical procedure and validation

Using the CFD program Ansys Fluent, the energy equation and melting model are numerically solved in three steps:

(1) The capsule space is treated as fluid PCM after creating its geometry.
(2) To keep the deviation to a minimum, the computational domain of different mesh elements of the network is determined and thus the required network is generated. For the studied case a convergence criterion of 10^{-6} is used.

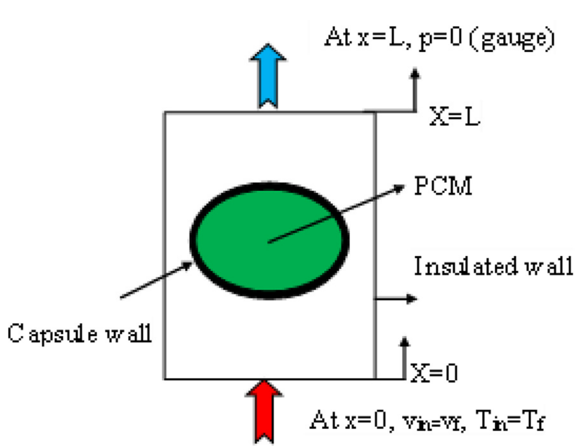

Fig. 2. Boundary conditions of the capsule.

(3) The axisymmetric 2-D physical parameters model is used for the PCM in the current work, where the energy stored is in two methods: heat latent and sensible heat. The sensible heat plays a significant role in places where the PCM temperature is above 331 K or below 329 K, while the latent heat is dominant between these two degrees.

The semi-implicit iteration (SIMPLE) approach is used to simultaneously solve the model's partial differential equations (PDEs). The energy and momentum equations are solved using second-order upwind techniques, and the pressure equation is rectified using the pressure option (PRESTO). At each time step, the convergence of the numerical solution was assessed using a convergence value of 10^{-6} (Soliman et al., 2022d, 2022e).

In this study, validation of the numerical model of melting is made through the comparison between the theoretical results of the present work and the experimental results of different capsules of Ref (Soliman et al., 2022a) of the same shape and dimensions as shown in Fig. 3. Fig. 3-a indicates the comparison between theoretical and experimental results for circular capsules, while Fig. 3-b indicates the same relation for the elliptical capsule.

The graphs demonstrate that the theoretical and experimental results generally agree. The correctness of the various thermal properties of paraffin wax and the validity of the theoretical model are both assured by the reasonable agreement between experimental and theoretical results.

3.3. Mesh dependency study

The current numerical model makes use of a free triangular mesh. With the temperature of the capsule starting at 300 K, a simulation is run for a circular capsule with a 4 cm diameter to look at how the numerical results depend on the size of the mesh elements. The capsule boundary is 343 K in temperature. Comparing the capsule liquid fraction and average temperature for various element sizes (20062, 32634, 45409, 68312, and 116774) reveals that a mesh size of 68312 is appropriate for the numerical model. A grid independence analysis has also been conducted for additional configurations in a similar

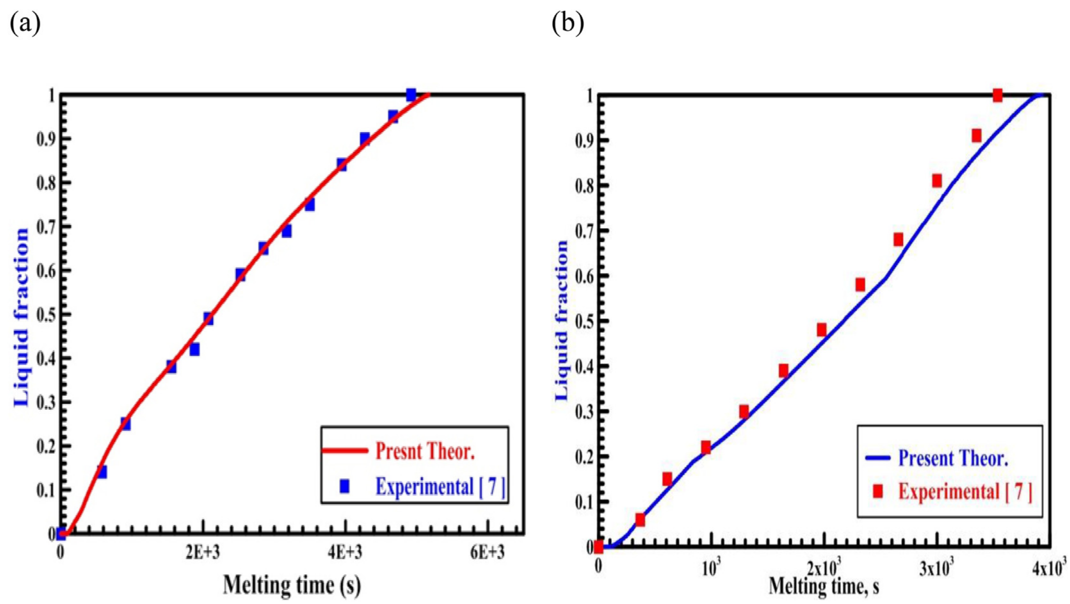

Fig. 3. Phase change material liquid fraction for (a) circular and (b) oval capsule vs. time for the present numerical study and experimental results of Ref (Soliman et al., 2022a).

manner. The analysis is performed in time steps of 0.5 s for all models (Fig. 4).

4. Results and discussion

In this section, the results of the ANSYS program for changing the size of the capsule are presented to show the effect of the capsule size on each of the liquid fractions, the temperature of the PCM, the total stored energy for each capsule, as well as the stored energy per kg of PCM and the efficiency of the storage system.

4.1. Comparison between the circular and elliptical capsule

Before proceeding with the discussion of the current results, the advantages of choosing an elliptical cross-section capsule over a circular cross-section capsule are established. Table 4 shows the liquid fraction contours for the circular and elliptical cross-sectional area of capsules. Both sections are subjected to the same conditions including the same cross-sectional area (the diameter of the circle is equal to 2 cm and the axes of the ellipse are 5 cm

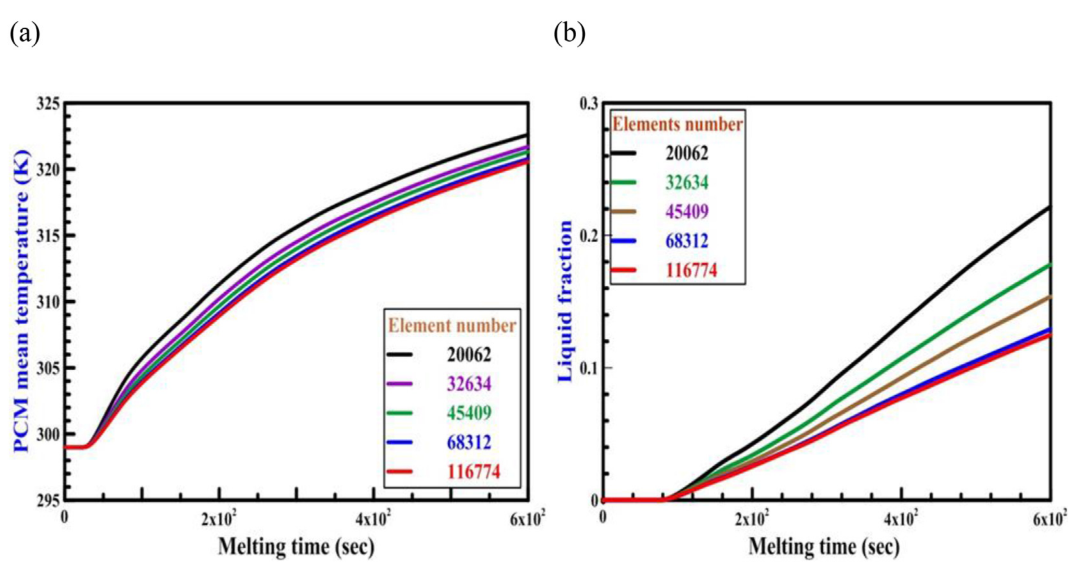

Fig. 4. Phase change material (a) temperature and (b) liquid fraction for circular capsule vs. time at different element size.

Table 4. Liquid fraction contours for the circular and elliptical capsules at the same cross-sectional area.

Circle capsule	Oval capsule
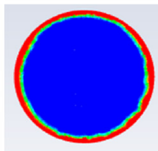 10 min	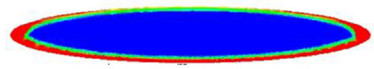
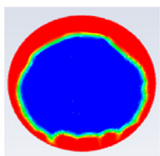 20 min	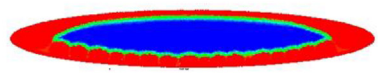
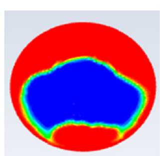 30 min	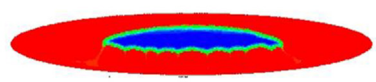
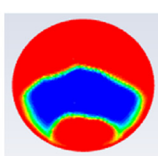 35 min	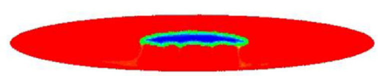
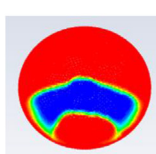 39 min	

horizontal and 0.8 cm vertical), with an HTF inlet temperature of 343 K and an inlet velocity of 0.003 m/s.

It is observed from the table that, the liquid fraction in the top part of the capsules is higher than the bottom part because of the buoyancy force. As the paraffin wax melts, it becomes less dense than the solid paraffin wax. This causes the melted paraffin wax to rise to the top of the capsule.

The oval capsule melts faster than the circular capsule because it has a larger contact area (the area of intersection between the capsule and the hot fluid) with the HTF. This is because the oval capsule has a longer perimeter than the circular capsule. The longer perimeter results in a larger surface area for heat transfer. The more accurate perimeter of the elliptical cross-section as a function of its axes using the Ramanujan second Approximation can be calculated as shown in the following equation (Soliman et al., 2022a):

$$C \approx \pi(a+b)\left(1+\frac{3\left(\frac{a-b}{a+b}\right)^2}{10+\sqrt{4-3\left(\frac{a-b}{a+b}\right)^2}}\right) \tag{18}$$

Fig. 5 indicates the effect of circular and elliptical sections on the relationship between the liquid fraction and the melting time. The figure shows that the two sections have the same liquid fraction of 1 at the end of the melting process but the time needed for the complete melting of an elliptical cross-section capsule is 2357 s, which is lower than that of the circular one, which takes 3557.5 s. The elliptical capsule melts faster because it has a larger contact area with the HTF. This is because the elliptical capsule has a longer perimeter than the circular capsule. The longer perimeter results in a larger surface area for heat transfer. The higher melting rate of the elliptical capsule means that it can store more power than the circular capsule for the same amount of PCM. This is because the power stored in a PCM-based thermal energy storage device is proportional to the melting rate.

This means that the performance of the elliptical capsule is better than the circular capsule. In other words, the power stored in the elliptical capsule is nearly 50 % greater than that of the circular capsule for the same amount of PCM.

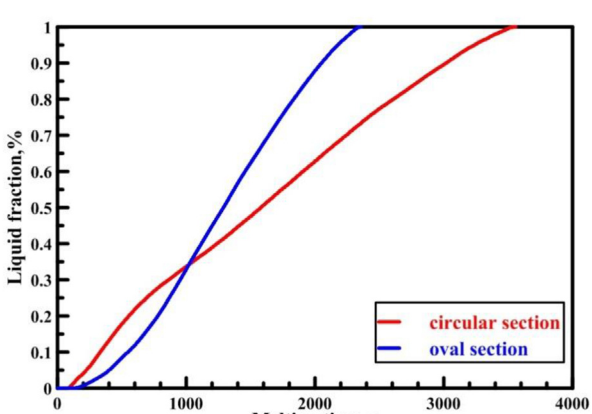

Fig. 5. Phase change material liquid fraction with time for elliptical and circular capsules at the same cross-sectional area.

4.2. Effect of capsules' volume ratio

In this subsection, we explore the effect of PCM V_r on melting time, PCM mean temperature, PCM liquid fraction, PCM total stored energy, and PCM stored energy per kg. Note that the volume ratio of the capsule means multiplying the volume of the initial capsule volume by several times (2, 3, 4, and 5).

4.2.1. PCM liquid fraction

Fig. 6 shows the PCM liquid fraction versus the melting time at a constant HTF velocity of 0.003, constant temperature of 343 K, and various values of volume ratio. One can see from the figure that the liquid fraction increases with time, at the same trend, for all values of the volume ratio. It can be seen from the figure also that all capsules of different volume ratios reach 100 % liquid fraction at different times, where the melting time increases with the volume fraction, as a result of the increasing mass of encapsulated PCM.

4.2.2. PCM mean temperature

Fig. 7 indicates the relation between mean PCM temperature and melting time at a constant HTF velocity of 0.003, the inlet temperature of 343 K, and different PCM volume ratios. It is seen from the figure that the mean PCM temperature increases with melting time until the beginning of the melting process, then it takes a nearly constant value during the process of melting and finally slightly increases during the PCM superheated period. Also, it is seen from the figure that the difference between the PCM temperatures of all volume ratio values is very small.

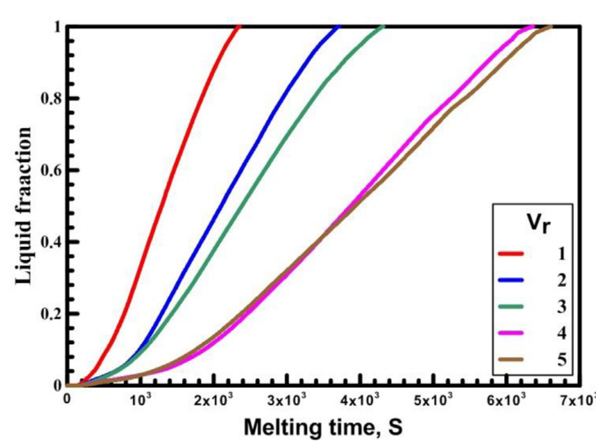

Fig. 6. Phase change material liquid fraction with time at different capsule volume ratios.

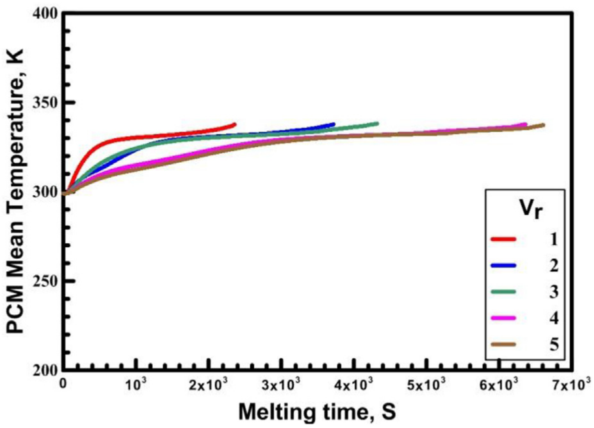

Fig. 7. Phase change material temperature with time at different capsule volume ratios.

4.2.3. PCM stored energy

The relationship between stored energy/kg of PCM and the melting time is presented in Fig. 8 at different values of capsule volume ratio. It is concluded from the figure that the stored energy increases with the melting time. After complete melting, the stored energy roughly has the same value for all cases, which means that the volume ratio of the PCM capsules has a slight effect on the energy stored/kg of PCM. It is shown also from the figure that the melting time decreases with volume ratio, which means that the smaller capsule, having a volume ratio of 1, is the best of all other capsules with a volume ratio higher than 1.

From the previous results, it becomes difficult to determine the absolute performance of the studied cases. Therefore, to indicate the best capsules, both the stored energy and the storage time must be taken into account. Dividing the stored energy of each capsule by the melting time of each capsule, we can conclude what is the best size for used capsules. Fig. 9 illustrates the relationship between PCM stored power per kg with the melting time. It can be seen from the figure that the capsule with a volume ratio of 1 has the highest power/kg, and the power decreases as the volume ratio increases. This means that the capsule with a volume ratio of 1 is the best size for PCM-based thermal energy storage devices in terms of power density. Power density is defined as the amount of power that can be stored per unit volume. A high power density is desirable for applications where a fast melting rate is required, such as in solar thermal energy storage systems.

4.3. Comparison between capsules of equal volume

To ensure that the capsule with the smallest size is the most efficient among the rest of the capsules, several calculations were made. These calculations are divided into two sections, in which the first section is a comparison between several capsules with a volume ratio of 1 so that its volume is equal to the size of one of the capsules whose volume ratio exceeds 1. The second group of calculations is concerned with calculating the exergy efficiency of all capsules with different volume ratios. Table 5 shows the liquid fraction contours for the oval capsule at double and quintuple volumes.

This group of results represents the comparison between several numbers of capsules with initial volume and one capsule with multiplication of volume (V_r). Fig. 10-a, b, c, and d shows the stored energy in the PCM over time for the two capsules with initial volume ($V_r = 1$), one capsule with double volume ($V_r = 2$), three capsules with initial volume ($V_r = 1$) and one capsule with triple volume ($V_r = 3$), four capsules with initial volume ($V_r = 1$) and one

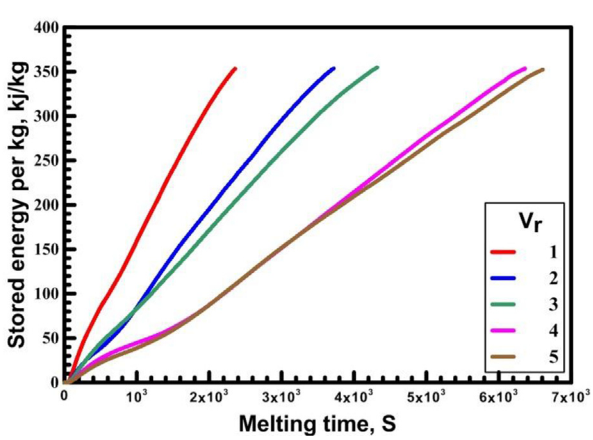

Fig. 8. Stored energy/kg of phase change material with time at different capsule volume ratios.

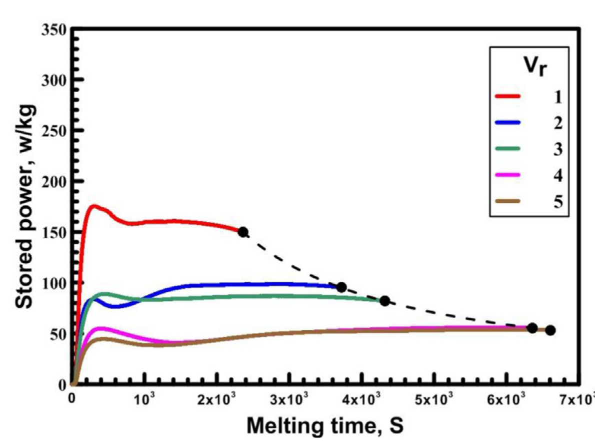

Fig. 9. Stored power per kg of phase change material with time at different capsule volume ratios.

Table 5. Liquid fraction contours for the oval capsule at double and quintuple volumes.

Double capsule		Quintuple capsule
		
0 min		
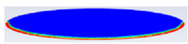	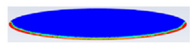	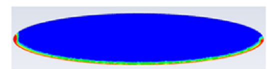
10 min		
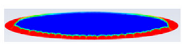	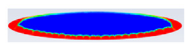	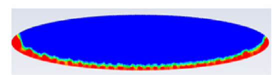
20 min		
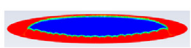	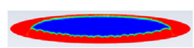	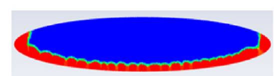
30 min		
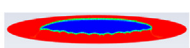	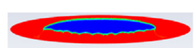	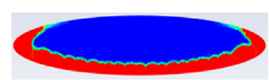
40 min		
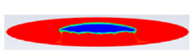	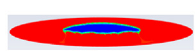	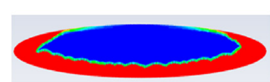
50 min		
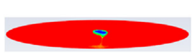	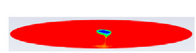	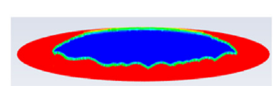
60 min		
		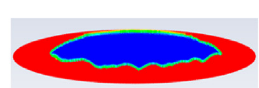
62 min		

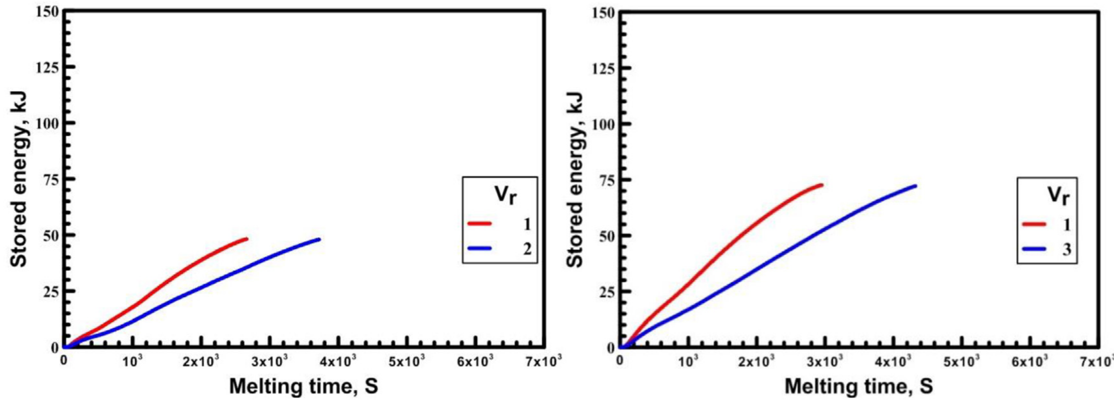

(a) Double-volume capsules and (b) triple-volume capsules

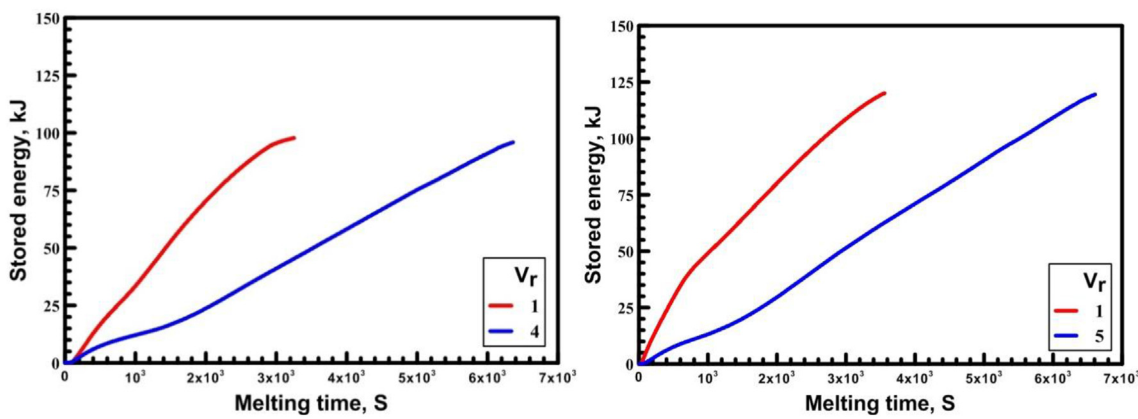

(c) Quadruple-volume capsules and(d) five-volume capsules

Fig. 10. Stored energy in phase change material and melting time for capsules of different volumes.

capsule with the quadruple volume ($V_r = 4$), and the five capsules with initial volume ($V_r = 1$) and one capsule with the quintuple volume ($V_r = 5$).

These figures show that using capsules with a volume ratio equal to 1 (the smallest size) always has a shorter melting time compared with capsules with multiple volumes. However, after complete melting, there is the same energy stored in the two configurations due to the same volume.

Therefore, the choice of the number of capsules and the volume ratio depends on the specific application. For applications where a fast-melting rate is required, different numbers of capsules at $V_r = 1$ can be used. For applications where a high energy density is required, one capsule with multiplying the initial volume can be used.

4.4. Encapsulated PCM exergy efficiency

Fig. 11 indicates the relationship between exergy efficiency and two sets of results. The first set concerns the capsules of different volume ratios (1, 2, 3, 4, and 5) concerning the smaller ones. The second set concerns the number of smallest capsules the volumes of which are equal to the volume of capsules with the different volume ratios of 1,2,3,4, and 5 capsules, respectively (the volume ratio of capsules and the number of capsules are the same in values). The figure shows that the exergy efficiency increases with increasing both the volume ratio and the number of capsules in the bundle. The exergy value in the case of volume ratio is higher than the value of the number of capsules. The exergy

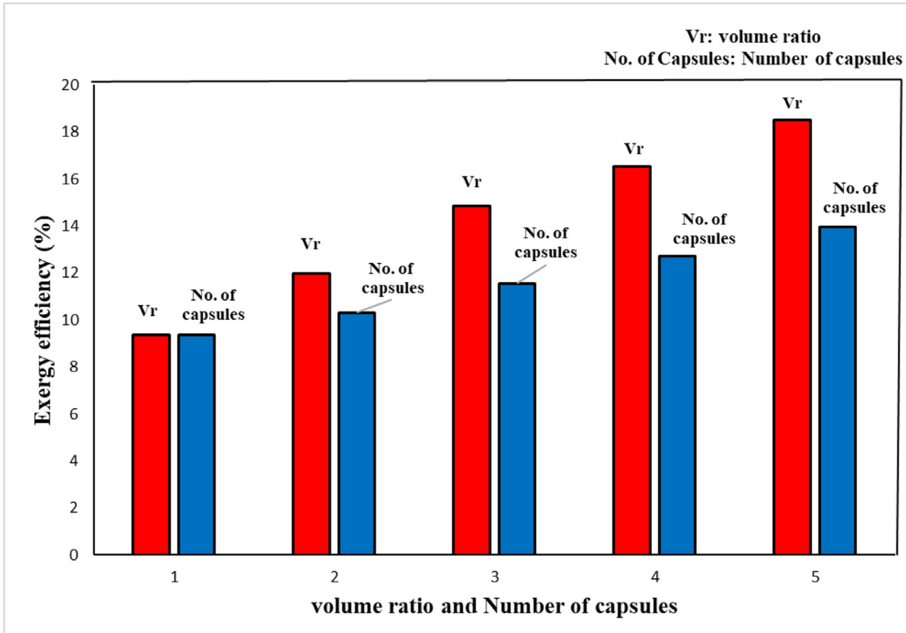

Fig. 11. Exergy efficiency versus volume ratio of capsules and number of capsules in bundles.

difference between the two configurations increases with the increase in the volume ratio and number of capsules. It is also seen that the capsule with a volume ratio equal to 5 has the highest exergy efficiency among all other capsules (18.5 %).

4.5. Conclusion

The melting process of the PCM in distinct storage capsule forms (circular and horizontal oval) that are heated by a constant wall temperature was explored numerically. The numerical model was developed to investigate the impact of the multiple numbers of capsules (2, 3, 4, and 5) as well as multiple V_r 1 capsule (including 2, 3, 4, and 5 volume) on the PCM melting process' thermal performance. Note that the volume ratio of the capsule means multiplying the volume of the initial capsule volume by several times (2, 3, 4, and 5). When the model was tested against earlier related research, the results indicated a good level of consistency. The following conclusions can be arrived at from the current numerical results of the PCM melting process inside various capsules:

(1) The performance of the elliptical cross-section of the capsule is higher than that of the circular section of the same cross-sectional area. Thus, the melting time decreases by up to 50 % for the same amount of heat stored in the capsule.
(2) Numerical outcomes of the PCM melting process are significantly influenced by the V_r value. The capsule melting time and its total energy stored increased as the value of V_r increased.
(3) The exergy difference between the two configurations (number of capsules and volume ratio) increases with the increase of the volume ratio and number of capsules.
(4) The exergy efficiency shows that the capsule with a V_r equal to 5 is the highest value among all the discussed capsules.

Author contribution

Ahmed Saad Soliman: concept, methodology, writing the original draft, validation, and computer programming. Ahmed A. Sultan: preparing literature survey, writing the initial draft, reviewing, editing, and supervision. Mohamed A. Sultan: literature survey preparation, computer programming, writing the initial draft, and editing.

Conflicts of interest

There are no conflicts of interest.

Acknowledgments

The authors express their gratitude to Mansoura University in Egypt for providing access to their facilities and for their assistance, which contributed to the advancement of their research.

References

Aadmi, M., Karkri, M., El Hammouti, M., 2015. Heat transfer characteristics of thermal energy storage for PCM (phase change material) melting in horizontal tube: numerical and experimental investigations. Energy 85, 339–352.

Abo-Elnour, F., Zeidan, E.B., Sultan, A.A., El-Negiry, E., Soliman, A.S., 2023. Enhancing the bifacial PV system by using dimples and multiple PCMs. J. Energy Storage 70, 108079.

Ali, M., Alkaabi, A.K., Addad, Y., 2022. Numerical investigation of a vertical triplex-tube latent heat storage/exchanger to achieve flexible operation of nuclear power plants. Int. J. Energy Res. 46, 2970–2987.

Dhaidan, N.S., 2021. Thermal performance of constrained melting of PCM inside an elliptical capsule of two orientations. Iran J. Sci. Technol. Trans. Mech. Eng. 45, 515–521.

Dhaidan, N.S., Khodadadi, J.M., Al-Hattab, T.A., Al-Mashat, S.M., 2013. Experimental and numerical study of constrained melting of n-octadecane with CuO nanoparticle dispersions in a horizontal cylindrical capsule subjected to a constant heat flux. Int. J. Heat Mass Tran. 67, 523–534.

Dinçer, İ., Rosen, M.A., 2010. Thermal Energy Storage Systems and Applications. Wiley. https://doi.org/10.1002/9780470970751.fmatter.

Dzikevics, M., Ansone, A., Blumberga, D., 2016. Modelling of phase change in spheres for applications in solar thermal heat storage systems. Energy Proc. 95, 112–118.

Goswami, Y.D., 2022. Principles of Solar Engineering. CRC Press, Boca Raton, 4th Edition. https://doi.org/10.1201/9781003244387.

Hajighafoori Boukani, N., Dadvand, A., Chamkha, A.J., 2018. Melting of a Nano-enhanced Phase Change Material (NePCM) in partially-filled horizontal elliptical capsules with different aspect ratios. Int. J. Mech. Sci. 149, 164–177.

Jamekhorshid, A., Sadrameli, S.M., Farid, M., 2014. A review of microencapsulation methods of phase change materials (PCMs) as a thermal energy storage (TES) medium. Renew. Sustain. Energy Rev. 31, 531–542.

Jegadheeswaran, S., Pohekar, S.D., Kousksou, T., 2010. Exergy based performance evaluation of latent heat thermal storage system: a review. Renew. Sustain. Energy Rev. 14, 2580–2595.

Kapilow, D., Hsuan, Y.G., Sun, Y., McCarthy, M., 2018. Convective melting and freezing of phase change materials encapsulated within small diameter polymer tubes. Exp. Therm. Fluid Sci. 92, 259–269.

Kothari, R., Sahu, S.K., Kundalwal, S.I., 2019. Comprehensive analysis of melting and solidification of a phase change material in an annulus. Heat Mass Tran. 55, 769–790.

Li, S., Chen, Y., Sun, Z., 2017. Numerical simulation and optimization of the melting process of phase change material inside horizontal annulus. Energies 10, 1249.

Li, M., Mahdi, J.M., Mohammed, H.I., Bokov, D.O., Mahmoud, M.Z., Naghizadeh, A., et al., 2021. Solidification enhancement in a multi-tube latent heat storage system for efficient and economical production: effect of number, position and temperature of the tubes. Nanomaterials 11, 3211.

Mahdi, M.S., Mahood, H.B., Khadom, A.A., Campbell, A.N., Hasan, M., Sharif, A.O., 2019. Experimental investigation of the thermal performance of a helical coil latent heat thermal energy storage for solar energy applications. Therm. Sci. Eng. Prog. 10, 287–298.

Öztürk, H.H., 2005. Experimental evaluation of energy and exergy efficiency of a seasonal latent heat storage system for greenhouse heating. Energy Convers. Manag. 46, 1523–1542.

Pássaro, J., Rebola, A., Coelho, L., Conde, J., Evangelakis, G.A., Prouskas, C., et al., 2022. Effect of fins and nanoparticles in the discharge performance of PCM thermal storage system with a multi pass finned tube heat exchange. Appl. Therm. Eng. 212, 118569.

Pirasaci, T., Wickramaratne, C., Moloney, F., Yogi Goswami, D., Stefanakos, E., 2017. Dynamics of phase change in a vertical PCM capsule in the presence of radiation at high temperatures. Appl. Energy 206, 498–506.

Rana, S., Zunaid, M., Kumar, R., 2022. Enhancement of thermal energy storage in a phase change material heat exchanger having elliptical and circular tubes with & without fins. J. Energy Storage 56, 105856.

Rosen, M.A., Dincer, I., 2003. Exergy methods for assessing and comparing thermal storage systems. Int. J. Energy Res. 27, 415–430.

Sabbaghi, S., Mehravar, S., 2015. Effect of using nano encapsulated phase change material on thermal performance of micro heat sink. Int. J. Nanosci. Nanotechnol. 11, 33–38.

Soliman, A.S., 2023. 4E analysis of a new design heat sink for cooling a bifacial photovoltaic system using PCM and ribs. J. Energy Storage 73, 108907.

Soliman, A.S., Zhu, S., Xu, L., Dong, J., Cheng, P., 2021a. Melting enhancement of nano-phase change material in cylindrical enclosure using convex/concave dimples: numerical simulation with experimental validation. J. Energy Storage 44, 103470.

Soliman, A.S., Zhu, S., Xu, L., Dong, J., Cheng, P., 2021b. Efficient waste heat recovery system for diesel engines using nano-enhanced phase change materials. Case Stud. Therm. Eng. 28, 101390.

Soliman, A.S., Zhu, S., Xu, L., Dong, J., Cheng, P., 2021c. Numerical simulation and experimental verification of constrained melting of phase change material in cylindrical enclosure subjected to a constant heat flux. J. Energy Storage 35, 102312.

Soliman, A.S., Zhu, S., Xu, L., Dong, J., Cheng, P., 2021d. Design of an H2O-LiBr absorption system using PCMs and powered by automotive exhaust gas. Appl. Therm. Eng. 191, 116881.

Soliman, A.S., Sultan, A.A., Sultan, M.A., 2022a. Effect of mushy zone parameter on phase change behavior of different configurations storage unit: numerical simulation and experimental validation. Sustainability 14, 14540.

Soliman, A.S., Xu, L., Dong, J., Cheng, P., 2022b. A novel heat sink for cooling photovoltaic systems using convex/concave dimples and multiple PCMs. Appl. Therm. Eng. 215, 119001.

Soliman, A.S., Radwan, A., Xu, L., Dong, J., Cheng, P., 2022c. Energy harvesting in diesel engines to avoid cold start-up using phase change materials. Case Stud. Therm. Eng. 31, 101807.

Soliman, A.S., Xu, L., Dong, J., Cheng, P., 2022d. Numerical investigation of the ribs' shape, spacing, and height on heat transfer performance of turbulent flow in a flat plate heat exchanger. Sustainability 14, 15143.

Soliman, A.S., Xu, L., Dong, J., Cheng, P., 2022e. Numerical investigation of a photovoltaic module under different weather conditions. Energy Rep. 8, 1045–1058.

Soliman, A.S., Fouda, M.S., Cheng, P., 2023. Power saving in a central air conditioning system by using multiple PCMs integrated with fresh air path. Energy Build. 300, 113691.

Sultan, M., Mostafa, H., El boz, A., Elngiry, E., 2021. Effect of inlet and geometrical parameters on the melting of PCM capsules of elliptical cross section. ERJ Eng. Res. J. 44, 11–20.

Vikas, Yadav, A., Samir, S., Arõcõ, M., 2022. A comprehensive study on melting enhancement by changing tube arrangement in a multi-tube latent heat thermal energy storage system. J. Energy Storage 55, 105517.

Watanabe, T., Kanzawa, A., 1995. Second law optimization of a latent heat storage system with PCMS having different melting points. Heat Recovery Syst. CHP 15, 641–653.